

# Ensemble Fluctuations of the Flux and Nuclear Composition of Ultra-High Energy Cosmic Ray Nuclei

Markus Ahlers,<sup>1</sup> Luis A. Anchordoqui,<sup>2</sup> and Andrew M. Taylor<sup>3</sup>

<sup>1</sup> Wisconsin IceCube Particle Astrophysics Center (WIPAC) and Department of Physics, University of Wisconsin, Madison, WI 53706, USA

<sup>2</sup> Department of Physics, University of Wisconsin-Milwaukee, Milwaukee, WI 53201, USA

<sup>3</sup> Dublin Institute for Advanced Studies, 31 Fitzwilliam Place, Dublin 2, Ireland

The flux and nuclear composition of ultra-high energy cosmic rays depend on the cosmic distribution of their sources. Data from cosmic ray observatories are yet inconclusive about their exact location or distribution, but provide a measure for the average local density of these emitters. Due to the discreteness of the emitters the flux and nuclear composition is expected to show ensemble fluctuations on top of the statistical variations, *i.e.* “cosmic variance”. This effect is strongest for the most energetic cosmic rays due to the limited propagation distance in the cosmic radiation background and is hence a local phenomenon. For the statistical analysis of cosmic ray emission models it is important to quantify the possible level of this variance. In this paper we present a completely analytic method that describes the variation of the flux and nuclear composition with respect to the local source density. We highlight that proposed future space-based observatories with exposures of  $\mathcal{O}(10^6 \text{ km}^2 \text{ sr yr})$  will attain sensitivity to observe these spectral fluctuations in the cosmic ray energy spectrum at Earth relative to the overall power-law fit.

PACS numbers: 96.50.S-, 98.70.Sa, 13.85.Tp

## I. INTRODUCTION

The nuclear composition of ultra-high energy (UHE) cosmic rays (CRs) is unknown and stands as one of the most challenging questions in particle astrophysics. Composition measurements can be made directly up to energies of about 100 TeV with space-based experiments [1]. For higher energies, the nuclear composition must be inferred from the extensive air shower (EAS) produced by the primary cosmic ray when it interacts in the upper atmosphere [2]. In order to collect the elusive events above  $10^{19.7} \text{ eV}$  (which present an integrated flux of less than 1 event per  $\text{km}^2$  per steradian and per century) observatories with large apertures and long exposure time are needed.

Today, the leading role is played by ground based facilities that cover vast areas with particle detectors overlooked by fluorescence telescopes. The largest is the Pierre Auger Observatory, with a surface detector array of 1600 water Cherenkov tanks covering  $3000 \text{ km}^2$ , which accumulates annually about  $6 \times 10^3 \text{ km}^2 \text{ sr yr}$  of exposure [3]. The more recently constructed Telescope Array (TA) covers  $700 \text{ km}^2$  with 507 scintillator detectors [4], which should accumulate annually about  $1.4 \times 10^3 \text{ km}^2 \text{ sr yr}$  of exposure.

In the near future, the JEM-EUSO mission will orbit the Earth on board the International Space Station at an altitude of about 400 km. Whilst in the “nadir” mode, the remote-sensing space instrument (with  $\pm 30^\circ$  field of view) will monitor an area of approximately  $1.3 \times 10^5 \text{ km}^2$ , recording video clips of fast UV flashes by sensing the fluorescence light produced through charged particle interactions. This innovative pathfinder mission

will observe approximately  $6 \times 10^4 \text{ km}^2 \text{ sr yr}$  annually [5], a factor of 10 above Auger.

At present, the best indicator of the nuclear composition is the atmospheric depth at which the shower develops its maximum size,  $X_{\max}$ . For a given shower, the position of  $X_{\max}$  depends on the depth of the first interaction in the atmosphere and the interaction step length of the cascade development. Thereby, it depends on the scattering cross section of the primary particle with air and on features of hadronic interactions at high energies. The average shower maximum,  $\langle X_{\max} \rangle$ , scales approximately as  $\ln(E/A)$ , where  $E$  is the energy and  $A$  is the atomic mass of the primary cosmic ray which generated the shower [6]. On average, the shower maximum for protons occurs deeper in the atmosphere than that for the same energy iron nucleus,  $\langle X_{\max}^p \rangle > \langle X_{\max}^{\text{Fe}} \rangle$ .

Further insight is expected to come from the magnitude of the root-mean-square (RMS) fluctuation of  $X_{\max}$ . If a group of showers is selected within a narrow range of energies, then fluctuations about the mean of  $X_{\max}$  (or in a parameter that is closely related to  $X_{\max}$  such as the steepness of the lateral distribution function or the spread of muon densities measured at ground) are expected to be larger for protons than for iron nuclei.

Unfortunately, because of the highly indirect method of measurement, extracting precise information from EASs has proved to be exceedingly difficult. The most fundamental problem is that the first generations of particles in the cascade are subject to large inherent fluctuations and consequently this limits the event-by-event energy resolution of the experiments. In addition, the center-of-mass energy of the first few cascade steps is well beyond any reached in collider experiments. There-

fore, one needs to rely on hadronic interaction models that attempt to extrapolate, using different mixtures of theory and phenomenology, our understanding of particle physics.

HiRes has presented evidence that the CR composition remains proton-like up to the highest energies [7]. The TA data are also compatible with proton primaries, but the statistics are still limited [8]. In contrast, Auger data on the depth of shower maximum, its RMS fluctuation, and muon rates at ground level indicate a transition of UHE CRs within the energy range  $10^{18}$  eV to  $10^{19.6}$  eV from a light (presumably proton-dominated) towards a heavier composition [9]. The apparent contradictory results reported by the HiRes, the Telescope Array, and the Pierre Auger collaborations suggest that known [10–12] and/or unknown systematic uncertainties may still affect the interpretation of EAS data.

Various features in the CR spectrum can also provide *indirect* evidence for the nuclear composition of UHE CRs. The *ankle* – a hardening of the spectrum at  $10^{18.5}$  eV – could be formed naturally by the superposition of two power-law fluxes and serves as a candidate of the transition between galactic heavy nuclei and extra-galactic cosmic ray protons [13, 14]. It has also been advocated that this feature could be well reproduced by a proton-dominated power-law spectrum, where the ankle is formed as a *dip* in the spectrum from the energy loss of protons via Bethe-Heitler pair production [15, 16]. In this case extra-galactic protons would already have started to dominate the spectrum beyond the *2nd knee*, a feature which corresponds to a slight *softening* of the spectrum at  $10^{17.7}$  eV.

Proton-dominance beyond the ankle is ultimately limited by the onset of photopion production on the cosmic microwave background (CMB), whereas dominance of a heavy composition is restricted by nucleus photodisintegration through the giant dipole resonance (GDR) [17, 18] – the so called *GZK-suppression* at around  $10^{19.7}$  eV. Indeed, a flux suppression in this energy region has been observed in the HiRes and Auger data with a high statistical significance [19–21]. As noted elsewhere [22, 23], secondary neutrinos and  $\gamma$ -rays of these hadronic interactions can serve as additional discriminators between various CR models. We will return to this interesting possibility in our conclusions.

In this paper we elaborate on the question as to what extent the spectral information in the GZK region can be used to discriminate between different CR source composition models. Due to the strength of the GZK mechanism the spectrum in this region is dominated by (and requires the presence of) local sources [24]. In this case the flux from a few CR sources can significantly fluctuate from a homogeneous distribution that is typically assumed in CR flux predictions [25]. In contrast to Poisson fluctuations in the GZK region [26] the manifestations of ensemble fluctuations persist in the limit of large event

statistics. We will quantify these stochastic fluctuations in the following utilizing an analytic solution to the flux of CR nuclei derived in Refs. [27, 28].

We will start in Sec. II with a brief review of the propagation of CR nuclei and the calculation of the mean observed fluxes. We discuss the analytic solution of the equation describing the flux from local CR sources in Sec. III. In Sec. IV these results will be used to derive an analytic approximation of the flux and mean mass variations due to the distribution of sources. We summarize our findings in Sec. V.

## II. PROPAGATION OF COSMIC RAY NUCLEI

Since cosmic rays are subject to deflections in galactic and inter-galactic magnetic fields the observed CR events do not point directly back to their sources. The identification of the CR sources is hence experimentally challenging and has so far proved inconclusive. There is a general consensus that the sources which are responsible of the UHE CR spectrum are of extra-galactic origin. These sources are expected to follow a spatially homogeneous distribution and the mean (ensemble-averaged) flux of UHE CRs (of type  $i$ ) follows a set of (Boltzmann) continuity equations of the form:

$$\begin{aligned} \dot{Y}_i = & \partial_E (H E Y_i) + \partial_E (b_i Y_i) - \Gamma_i^{\text{tot}} Y_i \\ & + \sum_j \int dE_j \gamma_{ji} Y_j + \mathcal{H} \mathcal{Q}_i, \end{aligned} \quad (1)$$

together with the Friedman-Lemaître equations describing the cosmic expansion rate  $H(z)$  as a function of red-shift  $z$ . We follow the usual cosmological *concordance model* dominated by a cosmological constant with  $\Omega_\Lambda \sim 0.7$  and a (cold) matter component,  $\Omega_m \sim 0.3$  where  $H^2(z) = H_0^2 [\Omega_m(1+z)^3 + \Omega_\Lambda]$ , normalized to its value today of  $H_0 \sim 70 \text{ km s}^{-1} \text{ Mpc}^{-1}$  [29]. The time-dependence of the red-shift can be expressed via  $dz = -dt/(1+z)H$ . The first and second terms on the r.h.s. of Eq. (1) describe, respectively, red-shift and other continuous energy losses (CEL) with rate  $b \equiv dE/dt$ . The third and fourth terms describe more general interactions involving particle losses ( $i \rightarrow \text{anything}$ ) with total interaction rate  $\Gamma_i^{\text{tot}}$ , and particle generation of the form  $j \rightarrow i$  with differential interaction rate  $\gamma_{ij}$ . The last term on the r.h.s. corresponds to the emission rate of CRs of type  $i$  per co-moving volume, depending on the emission rate  $\mathcal{Q}_i$  per source and their density  $\mathcal{H}$ .

The two main reactions of UHE CR nuclei during their cosmic evolution are photodisintegration [30–37] and Bethe-Heitler pair production [38] with the cosmic radiation background. In addition to the dominant contribution of the CMB we also include the infra-red/optical background from Ref. [39] in our calculation of interaction and energy loss rates. Photodisintegration is dominated by the GDR with main branches  $A \rightarrow (A-1) + N$

and  $A \rightarrow (A - 2) + 2N$  where  $N$  indicates a proton or neutron [31]. The GDR peak in the rest frame of the nucleus lies at about 20 MeV for one-nucleon emission, corresponding to  $E_{\text{GDR}}^A \simeq A \times 2 \times \epsilon_{\text{meV}}^{-1} \times 10^{19}$  eV in the cosmic frame with photon energies  $\epsilon = \epsilon_{\text{meV}}$  meV. At energies below 10 MeV there exist typically a number of discrete excitation levels that can become significant for low mass nuclei. Above 30 MeV, where the photon wavelength becomes comparable or smaller than the size of the nucleus, the photon interacts via substructures of the nucleus. Out of these the interaction with quasi-deuterons is typically most dominant and forms a plateau of the cross section up to the photopion production threshold at  $\sim 145$  MeV. Bethe-Heitler pair production can be treated as a continuous energy loss process with rate  $b_A(z, E) = Z^2 b_p(z, E/A)$ , where  $b_p$  is the energy loss rate of protons [38]. The (differential) photodisintegration rate  $\Gamma_{A \rightarrow B}(E)$  ( $\gamma_{A \rightarrow B}(E, E')$ ) is discussed in more detail in Ref. [28].

The evolution of the spectra proceeds very rapidly on cosmic time scales and the diffuse flux of secondary nuclei,  $J$ , looks generally quite different from the initial source injection spectrum [25]. The reaction network of nuclei depend in general on a large number of stable or long-lived isotopes. If the life-time of an isotope is much shorter than its photodisintegration rate it can be effectively replaced by its long-lived decay products in the network (1). Typically, neutron-rich isotopes  $\beta$ -decay to a stable or long-lived nucleus with the same mass number. In most cases there is only one stable nucleus per mass number below  $^{56}\text{Fe}$  with the exception of the pairs  $^{54}\text{Cr}/^{54}\text{Fe}$ ,  $^{46}\text{Ca}/^{46}\text{Ti}$ ,  $^{40}\text{Ar}/^{40}\text{Ca}$  and  $^{36}\text{S}/^{36}\text{Ar}$ . We follow here the approach of Ref. [31] (PSB) and consider only a single nucleus per mass number  $A$  in the decay chain of primary iron  $^{56}\text{Fe}$ . This PSB-chain of nuclei linked by one-nucleon losses is discussed in more detail in Ref. [28].

Note, that the set of Boltzmann Eqs. (1) does not take into account the deflection of charged CR nuclei during their propagation through magnetic fields. Magnetic scattering can be viewed as a diffusion process that depends on the particle's Larmor radius  $R_L = E/(ZeB) \simeq 1.1 \text{Mpc } E_{\text{eV}}/(ZB_{\text{nG}})$  and the coherence length of the magnetic field. At energies where the diffusion length becomes larger than the distance to the nearest CR source the CR spectrum is expected to be suppressed. It has been speculated that for particularly strong inter-galactic magnetic fields of strength  $\sim 1$  nG and coherence length of  $\sim 1$  Mpc (see *e.g.* Ref. [40]), the diffusive propagation of CR protons can start to affect the spectrum below about  $10^{18}$  eV [41]. For heavier nuclei diffusive propagation can in principle remain important up to higher energies due to the dependence  $R_L \propto 1/Z$  [42]. The results of this paper assume that the contribution of inter-galactic or galactic magnetic fields can be neglected for the calculation of the UHE CR spectrum.

As an example we show in Fig. 1 the solution of Eq. (1)

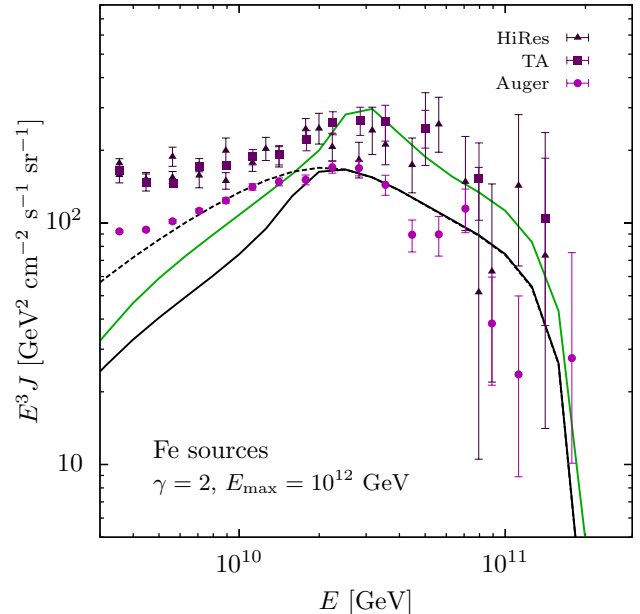


FIG. 1: The spectra from pure iron sources with exponential cutoff  $E_{\text{max}} = 10^{12}$  GeV and power index  $\gamma = 2$ . The green line shows the result of the analytic approximation for a homogeneous distribution of sources  $r_{\text{min}} < r < r_{\text{max}}$  with  $r_{\text{min}} = 10$  Mpc and  $r_{\text{max}} = 1$  Gpc. The solid black line is the corresponding numerical calculation including redshift scaling of interaction rates and energies. The dashed black line shows a model including sources up to  $z_{\text{max}} = 2$ . Also shown is recent data from HiRes [19], Auger [21] and the Telescope Array (TA) [43].

for an iron source model using a power-law spectral emission rate  $Q_{\text{Fe}} \propto E^{-\gamma} \exp(-E/E_{\text{max}})$  with  $\gamma = 2$  and  $E_{\text{max}} = 10^{21}$  eV. This model is motivated by a previous study [24] and reproduces the Auger data above the ankle within systematic uncertainties. The dashed black line corresponds to source contributions above  $r_{\text{min}} = 10$  Mpc extending up to redshift  $z_{\text{max}} = 2$  where no red-shift evolution of the emission is assumed, *i.e.*  $\mathcal{H} \propto 1$ . The solid black line marks the local contribution up to 1 Gpc calculated with the same method. This local contribution where red-shift scaling of energies and interaction rates is suppressed can be approximated by an analytic solution which is shown as the green solid line in the plot. We will discuss this method in the next section.

### III. ANALYTIC SOLUTION

Photodisintegration and photopion interactions of nuclei happen on timescales much shorter than the Hubble scale. Since we are interested in the variation of the average flux and mass composition from the distribution of local CR sources we will neglect redshift scalings in the following. In this case the Green's function of the Boltzmann equations (1) can be expressed in a simple analytic

form, as discussed in Refs. [27, 28].

The secondary nuclei produced via photodisintegration carry approximately the same Lorentz factor as the initial nucleus and the differential interaction rate in the set of Eqs. (1) can be approximated as  $\gamma_{A \rightarrow B}(E, E') \simeq \Gamma_{A \rightarrow B}(E)\delta(E' - (B/A)E)$ . It is hence convenient to express the energy of a nucleus with mass number  $A$  and red-shift  $z$  as  $AE$  where  $E$  denotes the energy *per nucleon*. Introducing the binned CR flux  $F_{A,i} \equiv \Delta E_i A dF_A(AE_i)/dE$ , and corresponding emission rates,  $Q_{A,i} \equiv A\Delta E_i Q_A(AE_i)$  we can re-write Eq. (1) in the compact form<sup>1</sup>

$$\frac{1}{r^2} \partial_r(r^2 F_{A,i}) \simeq \frac{\delta(r)}{4\pi r^2} Q_{A,i} - \sum_{B < A} \Gamma_{(A,i) \rightarrow (B,i)} F_{A,i} + \sum_{B > A} \Gamma_{(B,i) \rightarrow (A,i)} F_{B,i} + \Gamma_{A,i+1}^{\text{CEL}} F_{A,i+1} - \Gamma_{A,i}^{\text{CEL}} F_{A,i}, \quad (2)$$

where we define the rates:

$$\Gamma_{A,i}^{\text{CEL}} \equiv \frac{b_A(AE_i)}{A\Delta E_i}, \quad (3)$$

$$\Gamma_{(A,i) \rightarrow (B,i)} \equiv \Gamma_{A \rightarrow B}(AE_i). \quad (4)$$

In Ref. [28] it was shown that the general solution of Eq. (2), describing the flux from a source at distance  $r$  can be written in the form

$$F_{A,i}(r) \simeq \sum_{\mathbf{c}} \sum_{k=1}^{n_c} \mathcal{A}_k(\mathbf{c}) \frac{e^{-r\Gamma_{c_k}^{\text{tot}}}}{4\pi r^2} Q_{B,j}, \quad (5)$$

with dimensionless amplitudes

$$\mathcal{A}_k(\mathbf{c}) \equiv \prod_{l=1}^{n_c-1} \Gamma_{c_l \rightarrow c_{l+1}} / \prod_{p=1(\neq k)}^{n_c} \left( \Gamma_{c_p}^{\text{tot}} - \Gamma_{c_k}^{\text{tot}} \right), \quad (6)$$

where we sum over all possible production chains  $\mathbf{c} = \langle c_1, \dots, c_{n_c} \rangle$  with intermediate nuclei of mass number  $C$  in the energy bin  $k$  – denoted by the doublet  $c_i = (C, k)$  – and endpoints  $c_1 = (B, j)$ . The partial width  $\Gamma_{c_l \rightarrow c_{l+1}}$  includes nucleon-disintegration ( $\Gamma_{(A,i) \rightarrow (B,i)}$ ) as well as CEL ( $\Gamma_{(A,i) \rightarrow (A,i-1)}$ ).

In the following we will apply two more approximations to the solution (5) to reduce the number of terms. Firstly, we will reduce the CEL (last two terms on the r.h.s. of Eq. (2)) to the effective loss term

$$\Gamma_{A,i+1}^{\text{CEL}} F_{A,i+1} - \Gamma_{A,i}^{\text{CEL}} F_{A,i} \rightarrow -\frac{b_A(AE_i)}{AE_i} F_{A,i}. \quad (7)$$

This introduces a relative error of the order  $\partial_E(bEF)/(bF)$ , which is small in the relevant energy region of  $10^{18} - 10^{19}$  eV. And, secondly, we will only consider the one-nucleon loss chain of the PSB approximation. It was shown in Refs. [27, 28] that this is a good approximation for CR nuclei with a large mass number, which is the focus of this analysis.

#### IV. ENSEMBLE AVERAGE AND VARIATION

We now discuss the statistical variation of the CR flux and composition following Ref. [44]. Herein we assume that the probability distribution function (PDF) for local ( $r/H_0 \ll 1$ ) sources is flat in Euclidean space. Let  $n_s$  sources be distributed between redshift  $r_{\min}$  and  $r_{\max}$ . The number of sources can then be expressed via the (local) source density  $\mathcal{H}_0$  as  $n_s = \mathcal{H}_0(4\pi/3)(r_{\max}^3 - r_{\min}^3)$ . The PDF of a single source is given by

$$p(r) = \frac{\mathcal{H}_0}{n_s} 4\pi r^2 \Theta(r - r_{\min}) \Theta(r_{\max} - r). \quad (8)$$

The ensemble-average of a quantity  $A(r_1, \dots, r_{n_s})$  depending on the distance of the  $n_s$  sources can then be expressed as

$$\langle A \rangle = \int dr_1 \cdot \dots \cdot dr_{n_s} p(r_1) \cdot \dots \cdot p(r_{n_s}) A. \quad (9)$$

The ensemble-average of the local flux of CR nuclei given by  $\sum_{n_s} F_{A,i}(r_s)$  and Eq. (5) is simply

$$\langle N_{A,i} \rangle \equiv \mathcal{H}_0 \int_{r_{\min}}^{r_{\max}} dr' 4\pi r'^2 F_{A,i}(r'). \quad (10)$$

Using the abbreviation (6) we can then write this in an analytic form as

$$\langle N_{A,i} \rangle = \sum_{\mathbf{c}} \sum_{k=1}^{n_c} \mathcal{A}_k \xi(\Gamma_{c_k}^{\text{tot}}) Q_{c_{n_c}}, \quad (11)$$

where we define

$$\xi(\Gamma) \equiv \frac{\mathcal{H}_0}{\Gamma} (e^{-r_{\min}\Gamma} - e^{-r_{\max}\Gamma}). \quad (12)$$

From the experimental point of view the interesting quantities are the ensemble-averaged total flux of nuclei  $N_{\text{tot}}$  and mean mass number  $A_{\text{av}}$  at the highest CR energies  $E$ . The mean total flux is simply given by Eq. (11) as

$$\langle N_{\text{tot}}(E) \rangle \equiv \sum_A \langle N_A(E) \rangle. \quad (13)$$

We now return to the example of an iron source model shown in Fig. 1. The solid green line in Fig. 1 shows

<sup>1</sup> This form of the differential equation holds for nuclei heavier than beryllium. We can easily compensate for the process  ${}^9\text{Be} \rightarrow {}^4\text{He} + {}^4\text{He} + \text{n}$  of the PSB chain (see Ref. [28]) by re-defining  $F'_{A,i} = F_{A,i}/2$  for  $A = 2, 3, 4$  and  $F'_{A,i} = F_{A,i}$  for other nuclei. Similarly, the chains with nucleons as a final particle are re-weighted by the corresponding multiplicity in the case of intermediate nuclei lighter than  ${}^9\text{Be}$ .

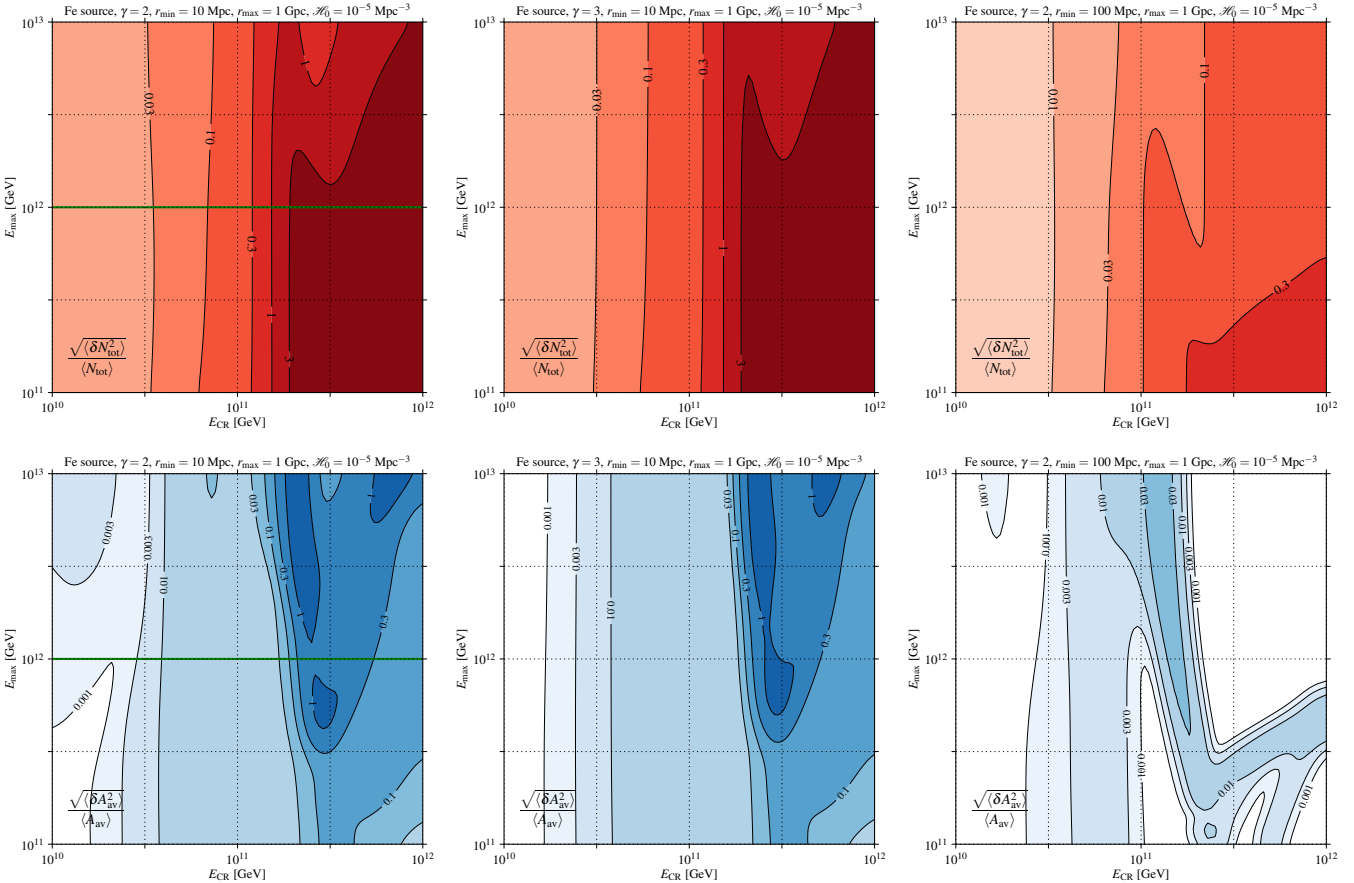


FIG. 2: The local relative error of the flux (Eq. (16); upper plots in red) and average mass composition (Eq. (18); lower plots in blue) for a distribution of iron sources with the model parameters indicated above the plots. The green line in the left plots indicate the corresponding relative error for the model shown in Fig. 1. All calculations assume a local source density of  $\mathcal{H}_0 = 10^{-5} \text{ Mpc}^{-3}$  and scale as  $\mathcal{H}_0^{-1/2}$ .

the result of the analytic approximation (11). This approximation agrees with the numerical result (solid black line) within a factor two or better depending on energy. The relative difference is expected from the onset of redshift scaling for propagation distances of the order of Gpc ( $z \simeq 1/4$ ). At low energies this introduces a relative upward shift of the flux of  $\simeq 30\%$  for a source model with  $\gamma = 2$  and  $\mathcal{H} \propto 1$ . This agrees well with the result of the calculations. In addition, threshold effects that lead to breaks in the spectrum scale with redshift as  $E_{\text{th}} \propto 1/(1+z)^2$  and are shifted to lower energies by up to  $\simeq 50\%$ . This effect can also be noticed by the relative position of the break in Fig. 1.

This example illustrates the limitations of the analytic solution for the calculation of large scale (early-time) contributions to the CR flux. However, the analytic approximation provides a convenient description of the nuclei cascades that happen on small scales and depend on the local source distribution. In particular, it enables us to study ensemble-variations of the flux. Using Eq. (6) we can write the variation of the CR flux in an explicit an-

alytic form as

$$\begin{aligned} \langle \delta N_{A,i} \delta N_{B,j} \rangle &\equiv \langle N_{A,i} N_{B,j} \rangle - \langle N_{A,i} \rangle \langle N_{B,j} \rangle \\ &= \sum_{\mathbf{c}, \bar{\mathbf{c}}} \sum_{k=1}^{n_c} \sum_{\bar{k}=1}^{n_{\bar{c}}} \mathcal{A}_k(\mathbf{c}) \mathcal{A}_{\bar{k}}(\bar{\mathbf{c}}) \zeta(\Gamma_{c_k}^{\text{tot}} + \Gamma_{\bar{c}_{\bar{k}}}^{\text{tot}}) Q_{c_{n_c}} Q_{\bar{c}_{n_{\bar{c}}}} \\ &\quad - \frac{1}{n_s} \langle N_{A,i} \rangle \langle N_{B,j} \rangle, \end{aligned} \quad (14)$$

where  $\zeta$  is defined as the expression

$$\zeta(\Gamma) \equiv \mathcal{H}_0 \int_{r_{\text{min}}}^{r_{\text{max}}} dr \frac{e^{-r\Gamma}}{4\pi r^2}. \quad (15)$$

Note that the last term in Eq. (14) is sometimes omitted since the number of sources  $n_s$  is expected to be large, but we keep it in our calculations. Based on these definitions we can express the relative variation of the total flux via the two-point density perturbations (14) as

$$\sigma_{\text{loc}}^2 = \sum_{A,B} \frac{\langle \delta N_A(E) \delta N_B(E) \rangle}{\langle N_{\text{tot}}(E) \rangle^2}. \quad (16)$$

$n$	$z_{\min}$	$z_{\max}$	$\gamma$	$n_s [10^6]$	$\sqrt{\sigma_{\text{adi}}^2} [\%]$
0	0.01	2	2	5.3	0.65
3	0.01	2	2	73	0.15
0	0.1	2	2	5.3	0.17
3	0.1	2	2	73	0.04
0	0.01	2	2.5	5.3	0.76
3	0.01	2	2.5	73	0.20
0	0.25	2	2	5.2	0.09
3	0.25	2	2	73	0.02
SFR ( $z_{\min} = 0.01$ )		2		173	0.14
SFR ( $z_{\min} = 0.01$ )		2.5		173	0.19

TABLE I: Estimated source number and adiabatic variation defined in Eqs. (19) and (21). We show results for a power-law cosmological evolution as  $\mathcal{H} = \mathcal{H}_0(1+z)^n$  with  $z_{\min} < z < z_{\max}$  and for the star formation rate (SFR) according to Ref. [45, 46] (with cutoff  $z_{\min} = 0.01$ ). In all cases we assume a local density of  $\mathcal{H}_0 = 10^{-5} \text{ Mpc}^{-3}$ .

With Eq. (13) we can also *define* the mean mass number as

$$\langle A_{\text{av}}(E) \rangle \equiv \sum_A \frac{A \langle N_A(E) \rangle}{\langle N_{\text{tot}}(E) \rangle}. \quad (17)$$

Note, that Eq. (17) is in the strict sense not the ensemble-average but serves as a first order estimator. For small fluctuations around the mean value we can approximate the relative variation of the mean mass number (17) via the two-point correlation function (14) as

$$\sigma_A^2 \simeq \sum_{B,C} \left( 1 - \frac{B}{\langle A_{\text{av}}(E) \rangle} \right) \left( 1 - \frac{C}{\langle A_{\text{av}}(E) \rangle} \right) \times \frac{\langle \delta N_B(E) \delta N_C(E) \rangle}{\langle N_{\text{tot}}(E) \rangle^2}. \quad (18)$$

In Figure 2 we show contour plots of the relative error of the flux (red; upper plots) and mass composition (blue; lower plots) for the case of iron sources with different model parameters indicated above the plots. The axis show the observed CR energy vs. the exponential cutoff energy  $E_{\text{max}}$ . For the calculation we introduced logarithmic energy bins of  $\Delta \log_{10} E/\text{GeV} = 0.02$  and smoothed the result with a Gaussian kernel to account for an experimental resolution of 0.1. This procedure smoothes out features in the relative variance that are beyond the experimental resolution and result from the rapid nuclei transitions in the GZK region in combination with the relative CR energy shift with the mass of the daughter nuclei.

The results do not strongly depend on the spectral index as can be seen for the cases  $\gamma = 2$  and  $\gamma = 3$  with otherwise equal parameters that are shown in the plots of the first two columns. This set of plots assumes

a local distribution between 10 Mpc and 1 Gpc. The relative errors are significantly reduced as we increase the distance to the closest source to 100 Mpc as shown in the plots of the last column in Fig. 2. However, this is only marginally reproducing the UHE CR spectrum as pointed out in Ref. [24]. Note that the green lines in the plots of the left column mark the contribution for the iron source model with  $E_{\text{max}} = 10^{21} \text{ eV}$  considered in Fig. 1.

One can also notice from the lower plots of Fig. 2 that the relative error of the average mass composition is below 1% for CR energies below  $10^{19.5} \text{ eV}$ . This energy marks the end of the energy region where CR event statistics allow an inference of the mass composition from CR data as described in the introduction. Note that all the plots in Fig. 2 show the case of a local source density of  $\mathcal{H}_0 = 10^{-5} \text{ Mpc}^{-3}$  and levels increase as  $\mathcal{H}_0^{-1/2}$ . Hence, even for a density  $\mathcal{H}_0 = 10^{-6} \text{ Mpc}^{-3}$ , still marginally consistent with the data, the ensemble fluctuation on the average mass composition probed by present generation experiments may be safely neglected.

So far we have considered the case that  $\Gamma/H_0 \ll 1$  valid at the highest CR energies where we can neglect cosmological contributions of the sources and treat the problem as effectively local. In the opposite case,  $\Gamma/H_0 \gg 1$ , it is also possible to give an analytic expression of the statistical variation of the CR flux. We assume that  $n_s$  sources are isotropically distributed between redshift  $z_{\min}$  and  $z_{\max}$  with comoving density  $\mathcal{H}(z)$ , and local density  $\mathcal{H}_0$ . The number of sources is then given by

$$n_s = \int dz \frac{d\mathcal{V}}{dz} \mathcal{H}(z) = \int \frac{dz}{H(z)} 4\pi d_C^2(z) \mathcal{H}(z) \quad (19)$$

where the comoving volume is  $\mathcal{V}_C(z) = (4\pi/3)d_C^3(z)$  with comoving distance (in a flat universe)  $d_C(z) = \int_0^z dz'/H(z')$ . The PDF of a single source as a function of redshift is then a simple generalization of Eq. (8),

$$p(z) = \frac{1}{H(z)} \frac{\mathcal{H}(z)}{n_s} 4\pi d_C^2(z). \quad (20)$$

As long as only adiabatic redshift scaling is involved the flux of a single source is given by  $dF/dE = \mathcal{Q}((1+z)E)/(4\pi d_C^2)$ . Assuming  $\mathcal{Q}(E) \propto E^{-\gamma}$  we then obtain a relative variation of

$$\sigma_{\text{adi}}^2 = \frac{\int dz p(z) [(1+z)^{-\gamma}/d_C^2(z)]^2}{[\int dz p(z)(1+z)^{-\gamma}/d_C^2(z)]^2} - \frac{1}{n_s}. \quad (21)$$

We show values for  $n_s$  and  $(\sigma_{\text{adi}}^2)^{1/2}$  in Tab. I. Obviously, the statistical variation of the average mass number is negligible in this regime.

The two limiting behaviors of the relative flux variation (16) and (21) motivates the following treatment of the overall relative flux variation. Using the numerical result of the set of Boltzmann Eqs. (1) we can calculate the

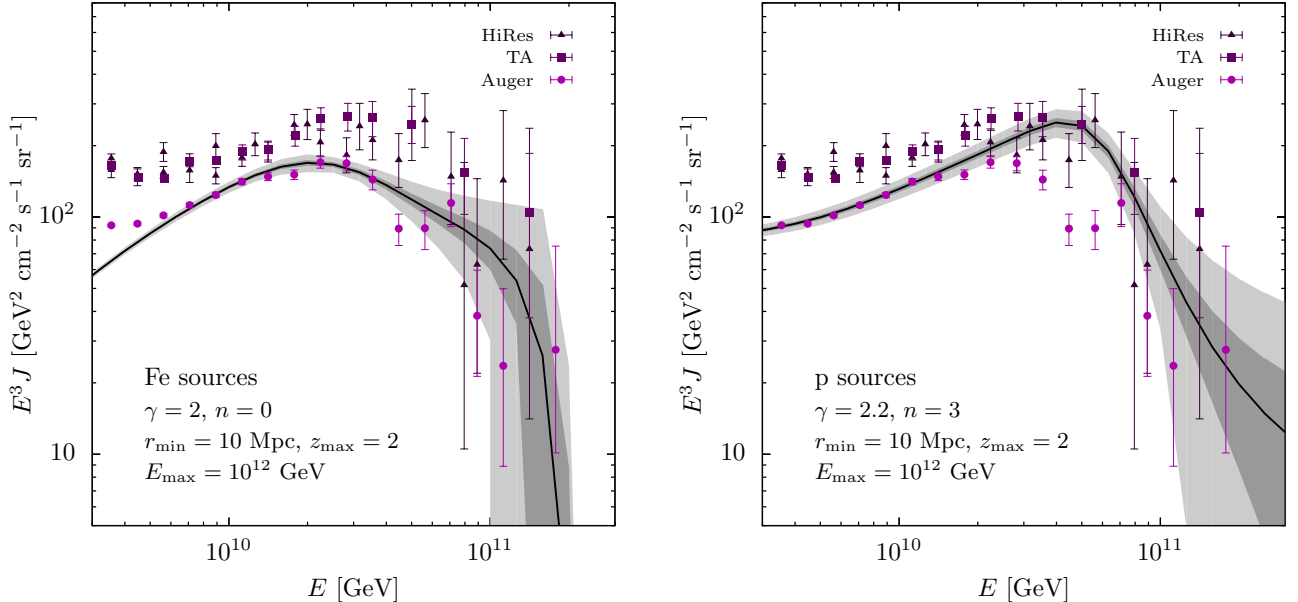


FIG. 3: **Left panel:** The example of Fig. 1 including the approximate variation of the flux assuming a local source distribution  $\mathcal{H}_0 = 10^{-5} \text{ Mpc}^{-3}$  (dark gray band) and  $\mathcal{H}_0 = 10^{-6} \text{ Mpc}^{-3}$  (light gray band). **Right panel:** For comparison, a proton model with similar source parameters.

average flux for the local ( $r \lesssim 1 \text{ Gpc}$ ), and global source distribution. This corresponds to the solid and dashed lines, respectively, in Fig. 1. The flux variation can then be approximated via the superposition

$$\sigma_N^2(E) \simeq (1-x)^2 \sigma_{\text{adi}}^2 + x^2 \sigma_{\text{loc}}^2(E), \quad (22)$$

where  $\sigma_{\text{loc}}^2$  is calculated from the analytic approximation (16),  $\sigma_{\text{adi}}^2$  the adiabatic limit (21) for  $r_{\text{min}} \simeq 1 \text{ Gpc}$  ( $z_{\text{min}} \simeq 0.25$ ) and  $x = \langle N_{\text{loc}}(E) \rangle / \langle N_{\text{global}}(E) \rangle$  from the numerical evaluation.

In the left plot of Fig. 3 we show the result of this procedure for the previous example of iron sources shown in Fig. 1. The solid line (corresponding to the dashed line in Fig. 1) shows the contribution from the cosmological distribution of iron sources. The shaded areas show the flux within its variation based on Eq. (22) for a local source density  $\mathcal{H}_0 = 10^{-5} \text{ Mpc}^{-3}$  (dark gray) and  $\mathcal{H}_0 = 10^{-6} \text{ Mpc}^{-3}$  (light gray). A local source density of  $\mathcal{H}_0 = 10^{-5} \text{ Mpc}^{-3}$  is consistent with the absence of “repeaters” in CR data [47, 48]. Note, that the relative size of the error bands increases as  $\mathcal{H}_0^{-1/2}$ . Values as low as  $\mathcal{H}_0 = 10^{-6} \text{ Mpc}^{-3}$  are still marginally consistent with auto-correlation studies of UHE CR nuclei [49].

The right plot of Fig. 3 shows the corresponding result of a proton source model with similar source parameters. The amplitude of the ensemble fluctuation is comparable to the case of iron and does not serve as a direct measure of the source composition. However, the spectral feature of the GZK-suppression is significantly different to the case of the iron model. In particular, the iron source model experiences a much steeper suppression at the upper end of the UHE CR spectrum. This

poses a challenge to account for the most extreme UHE events like the  $3 \times 10^{20} \text{ eV}$  Fly’s Eye event [50], if sources are too distant [24]. Candidate nearby sources of heavy nuclei include starburst galaxies [51] and ultra-fast spinning newly-born pulsars [52, 53]. Our method provides a tool to distinguish ensemble fluctuations from spectral features of the the average source contribution on a statistical basis.

Proposed future space-based CR observatories can reach integrated exposures of  $\mathcal{O}(10^6 \text{ km}^2 \text{ s yr})$  [54]. This is a factor of about 100 larger than the integrated exposure reached by present ground-based air shower arrays. The statistical error of UHE CR measurements can thus be improved by a factor 10. With such a resolution the observed UHE CR spectrum can show a significant deviation from the ensemble mean due to the discreteness of close-by source contributions. For instance, the spectrum could exhibit “spectral wiggles” beyond the GZK suppression. Our method describes a way to quantify the bin-to-bin amplitude of these modulations for the case of a ultra-high energy cosmic ray nuclei.

## V. CONCLUSIONS

In this paper we have studied the ensemble fluctuations of the mean flux and average mass number of UHE CR nuclei from the distribution of sources. We have derived an analytic expression for the relative errors which applies to the CR data at the highest energies dominated by the local sub-Gpc (low redshift) source distribution.

For lower energies another analytic approximation can be derived through the use of adiabatic scaling of the source contributions. This method can be easily generalized to the case of ensemble fluctuations due to the source emission parameters such as the spectral index and the maximal energy.

As an illustration, we applied these results to a fiducial iron source model for which a homogeneous distribution of sources had previously been found to successfully reproduce the CR data within systematic uncertainties. For the case of a local source density  $\mathcal{H}_0 = 10^{-5} \text{ Mpc}^{-3}$ , the resultant ensemble fluctuations of the average mass composition on top of the ensemble mean were found to exist at a tolerable level for the analysis of present generation CR composition data below  $10^{19.5} \text{ eV}$ .

However, the level of ensemble fluctuations for present generation spectral studies of the GZK suppression are potentially not ignorable if a smaller source density of  $\mathcal{H}_0 = 10^{-6} \text{ Mpc}^{-3}$  is assumed, which still remains marginally consistent with angular correlation studies. In general, the amplitude of the ensemble fluctuations of the flux does not serve as a direct discriminator between CR models with different source compositions. This is apparent in the comparison between the iron and proton source models in Fig. 3. However, our study does provide an analytic method to quantify these ensemble variations enabling one to distinguish them from the GZK-suppression effect of the mean flux in a statistical way. Indeed, unless the actual source densities are much larger than those considered here, next generation experiments reaching accumulated exposures  $\mathcal{O}(10^6 \text{ km}^2 \text{ sr yr})$  should be sufficiently sensitive to potentially discern these fluctuations.

In addition to their spectral signatures, the hadronic interactions responsible for the GZK suppression are associated with a high-energy flux of *cosmogenic* neutrinos [55–63] and  $\gamma$ -rays [64–66], following from photopion production of nucleons and subsequent decay. In addition, photodisintegration of high-energy nuclei can be followed by immediate photo-emission from excited daughter nuclei [67] as well as neutrino-emission from  $\beta$ -decay of the secondaries [68, 69].

While the presence of a suppression feature in the spectrum is generally expected for all compositions, the flux of cosmogenic neutrinos and  $\gamma$ -rays subsequently produced are both very sensitive to the CR source model. Indeed this difference permits information on these fluxes to be used as a probe of the composition or vice-versa. For instance, an upper limit on the proton fraction in

UHE extra-galactic CRs can, in principle, be inferred from experimental bounds on both the diffuse flux of UHE neutrinos [22] and the diffuse flux of UHE photons [23]. Furthermore, these two messengers starkly contrast in their subsequent propagation, with UHE neutrinos freely propagating out to the Hubble-scale whereas UHE  $\gamma$ -rays being limited to tens of Mpc distance scales. This difference of scales highlights the fact that these two messengers can offer complementary information about the distant and local source distribution respectively.

Moreover, the accompanying output into secondary electrons and positrons, in particular from Bethe-Heitler pair production, feeds into electromagnetic cascades in the CMB and intergalactic magnetic fields. This leads to the accumulation of  $\gamma$ -rays at GeV-TeV energies. The observed diffuse  $\gamma$ -ray flux by Fermi-LAT [70] thus provides a constraint on the total energy injected into such cascades over the Universe’s entire history and can be translated into upper limits on the cosmic diffuse flux of photons and neutrinos [71–73].

In conclusion, future space-based observatories with colossal exposures,  $\mathcal{O}(10^6 \text{ km}^2 \text{ sr yr})$ , will provide the required large statistics at the high-energy end of the CR spectrum, allowing to separate ensemble fluctuation from the GZK suppression features on a statistical basis. In combination with information on the arrival-direction distribution of CRs and on the secondary fluxes of  $\gamma$ -rays and neutrinos these spectral features can provide a coherent picture for an *indirect* determination of the UHE CR nuclear composition [74] and will naturally complement the current *direct* measurements of EAS observables.

## Acknowledgments

MA acknowledges support by a John Bahcall Fellowship for neutrino astronomy of the Wisconsin IceCube Particle Astrophysics Center (WIPAC) and by the U.S. National Science Foundation (NSF) under grants OPP-0236449 and PHY-0236449. LAA is supported by the NSF under CAREER Grant PHY-1053663, the National Aeronautics and Space Administration (NASA) Grant 11-APRA11-0058, and the UWM Research Growth Initiative. AMT acknowledges support by a Schroedinger Fellowship at Dublin Institute for Advanced Study. Any opinions, findings, and conclusions or recommendations expressed in this material are those of the authors and do not necessarily reflect the views of NASA or NSF.

---

[1] H. S. Ahn, P. Allison, M. G. Bagliesi, J. J. Beatty, G. Bigongiari, J. T. Childers, N. B. Conklin and S. Couto *et al.*, *Astrophys. J.* **714**, L89 (2010) [arXiv:1004.1123 [astro-ph.HE]].

[2] L. Anchordoqui, M. T. Dova, A. G. Marazza, T. McCauley, T. C. Paul, S. Reucroft and J. Swain, *Annals Phys.* **314**, 145 (2004) [arXiv:hep-ph/0407020].

[3] J. Abraham *et al.* [Pierre Auger Collaboration], *Nucl.*

Instrum. Meth. A **613**, 29 (2010) [arXiv:1111.6764 [astro-ph.IM]].

[4] T. Abu-Zayyad *et al.* [Telescope Array Collaboration], Nucl. Instrum. Meth. A **689**, 87 (2012) [arXiv:1201.4964 [astro-ph.IM]].

[5] J. H. Adams Jr. *et al.*, [arXiv:1203.3451 [astro-ph.IM]].

[6] J. Linsley and A. A. Watson, Phys. Rev. Lett. **46**, 459 (1981).

[7] R. U. Abbasi *et al.* [HiRes Collaboration], Phys. Rev. Lett. **104**, 161101 (2010) [arXiv:0910.4184 [astro-ph.HE]].

[8] Y. Tsunesada [for the Telescope Array Collaboration], Proceedings of ICRC2011, Beijing [arXiv:1111.2507 [astro-ph.HE]].

[9] J. Abraham *et al.* [Pierre Auger Collaboration], Phys. Rev. Lett. **104**, 091101 (2010) [arXiv:1002.0699 [astro-ph.HE]].

[10] G. Wilk and Z. Wlodarczyk, J. Phys. G G **38**, 085201 (2011) [arXiv:1006.1781 [astro-ph.HE]].

[11] A. D. Supanitsky and G. Medina-Tanco, J. Phys. G G **39**, 095203 (2012) [arXiv:1206.7089 [astro-ph.IM]].

[12] L. Cazon and R. Ulrich, [arXiv:1203.1781 [astro-ph.IM]].

[13] J. Linsley, *Proceedings of ICRC 1963, Jaipur, India*, (Commercial Printing Press, Ltd., Bombay, India, 1964), pp. 77-99.

[14] C. T. Hill and D. N. Schramm, Phys. Rev. D **31**, 564 (1985).

[15] M. Hillas, Phys. Lett. A **24**, 677 (1967).

[16] V. Berezinsky, A. Z. Gazizov and S. I. Grigorieva, Phys. Rev. D **74**, 043005 (2006) [arXiv:hep-ph/0204357].

[17] K. Greisen, Phys. Rev. Lett. **16**, 748 (1966).

[18] G. T. Zatsepин and V. A. Kuzmin, JETP Lett. **4**, 78 (1966) [Pisma Zh. Eksp. Teor. Fiz. **4**, 114 (1966)].

[19] R. Abbasi *et al.* [HiRes Collaboration], Phys. Rev. Lett. **100**, 101101 (2008) [arXiv:astro-ph/0703099].

[20] J. Abraham *et al.* [Pierre Auger Collaboration], Phys. Rev. Lett. **101**, 061101 (2008) [arXiv:0806.4302 [astro-ph]].

[21] J. Abraham *et al.* [Pierre Auger Collaboration], Phys. Lett. B **685**, 239 (2010) [arXiv:1002.1975 [astro-ph.HE]].

[22] M. Ahlers, L. A. Anchordoqui and S. Sarkar, Phys. Rev. D **79**, 083009 (2009) [arXiv:0902.3993 [astro-ph.HE]].

[23] D. Hooper, A. M. Taylor and S. Sarkar, Astropart. Phys. **34**, 340 (2011) [arXiv:1007.1306 [astro-ph.HE]].

[24] A. M. Taylor, M. Ahlers and F. A. Aharonian, Phys. Rev. D **84**, 105007 (2011) [arXiv:1107.2055 [astro-ph.HE]].

[25] L. A. Anchordoqui, M. T. Dova, L. N. Epele and J. D. Swain, Phys. Rev. D **57**, 7103 (1998) [arXiv:astro-ph/9708082].

[26] D. De Marco, P. Blasi and A. V. Olinto, Astropart. Phys. **20**, 53 (2003) [arXiv:astro-ph/0301497].

[27] D. Hooper, S. Sarkar and A. M. Taylor, Phys. Rev. D **77**, 103007 (2008) [arXiv:0802.1538 [astro-ph]].

[28] M. Ahlers and A. M. Taylor, Phys. Rev. D **82**, 123005 (2010) [arXiv:1010.3019 [astro-ph.HE]].

[29] J. Beringer *et al.* [Particle Data Group], Phys. Rev. D **86**, 010001 (2012).

[30] F. W. Stecker, Phys. Rev. **180**, 1264 (1969).

[31] J. L. Puget, F. W. Stecker and J. H. Bredekamp, Astropys. J. **205**, 638 (1976).

[32] L. N. Epele and E. Roulet, JHEP **9810**, 009 (1998) [arXiv:astro-ph/9808104].

[33] J. P. Rachen, *Interaction processes and statistical properties of the propagation of cosmic-rays in photon backgrounds*, PhD thesis of the Bonn University, 1996.

[34] F. W. Stecker and M. H. Salamon, Astrophys. J. **512**, 521 (1999) [arXiv:astro-ph/9808110].

[35] E. Khan *et al.*, Astropart. Phys. **23**, 191 (2005) [arXiv:astro-ph/0412109].

[36] D. Allard, E. Parizot, E. Khan, S. Goriely and A. V. Olinto, Astron. Astrophys. **443**, L29 (2005) [arXiv:astro-ph/0505566].

[37] S. Goriely, S. Hilaire and A. J. Koning, Astron. Astrophys. **487**, 767 (2008) [arXiv:0806.2239 [astro-ph]].

[38] G. R. Blumenthal, Phys. Rev. D **1**, 1596 (1970).

[39] A. Franceschini, G. Rodighiero and M. Vaccari, Astron. Astrophys. **487**, 837 (2008) [arXiv:0805.1841 [astro-ph]].

[40] P. P. Kronberg, Rept. Prog. Phys. **57**, 325 (1994).

[41] R. Aloisio and V. S. Berezinsky, Astrophys. J. **625**, 249 (2005) [arXiv:astro-ph/0412578].

[42] D. Harari, S. Mollerach and E. Roulet, JHEP **9908**, 022 (1999) [arXiv:astro-ph/9906309].

[43] T. Abu-Zayyad *et al.* [Telescope Array Collaboration], [arXiv:1205.5067 [astro-ph.HE]].

[44] M. A. Lee, Astrophys. J. **229**, 424 (1979).

[45] A. M. Hopkins and J. F. Beacom, Astrophys. J. **651**, 142 (2006) [arXiv:astro-ph/0601463].

[46] H. Yuksel, M. D. Kistler, J. F. Beacom and A. M. Hopkins, Astrophys. J. **683**, L5 (2008) [arXiv:0804.4008 [astro-ph]].

[47] E. Waxman, K. B. Fisher and T. Piran, Astrophys. J. **483**, 1 (1997) [arXiv:astro-ph/9604005].

[48] T. Kashti and E. Waxman, JCAP **0805**, 006 (2008) [arXiv:0801.4516 [astro-ph]].

[49] H. Takami, S. Inoue and T. Yamamoto, Astropart. Phys. **35**, 767 (2012) [arXiv:1202.2874 [astro-ph.HE]].

[50] D. J. Bird, Astrophys. J. **441**, 144 (1995) [arXiv:astro-ph/9410067].

[51] L. A. Anchordoqui, G. E. Romero and J. A. Combi, Phys. Rev. D **60**, 103001 (1999) [arXiv:astro-ph/9903145].

[52] P. Blasi, R. I. Epstein and A. V. Olinto, Astrophys. J. **533**, L123 (2000) [arXiv:astro-ph/9912240].

[53] K. Fang, K. Kotera and A. V. Olinto, Astrophys. J. **750**, 118 (2012) [arXiv:1201.5197 [astro-ph.HE]].

[54] A. Santangelo and A. Petrolini, New J. Phys. **11**, 065010 (2009) [arXiv:0909.5370 [astro-ph.HE]].

[55] V. S. Berezinsky and G. T. Zatsepин, Phys. Lett. B **28**, 423 (1969).

[56] F. W. Stecker, Astrophys. J. **228**, 919 (1979).

[57] S. Yoshida and M. Teshima, Prog. Theor. Phys. **89**, 833 (1993).

[58] R. J. Protheroe and P. A. Johnson, Astropart. Phys. **4**, 253 (1996) [arXiv:astro-ph/9506119].

[59] R. Engel, D. Seckel and T. Stanev, Phys. Rev. D **64**, 093010 (2001) [arXiv:astro-ph/0101216].

[60] Z. Fodor, S. D. Katz, A. Ringwald and H. Tu, JCAP **0311**, 015 (2003) [arXiv:hep-ph/0309171].

[61] L. A. Anchordoqui, H. Goldberg, D. Hooper, S. Sarkar and A. M. Taylor, Pierre Auger Observatory,” Phys. Rev. D **76**, 123008 (2007) [arXiv:0709.0734 [astro-ph]].

[62] K. Kotera, D. Allard and A. V. Olinto, JCAP **1010**, 013 (2010) [arXiv:1009.1382 [astro-ph.HE]].

[63] M. Ahlers and F. Halzen, [arXiv:1208.4181 [astro-ph.HE]].

[64] G. Gelmini, O. E. Kalashev and D. V. Semikoz, Astropart. Phys. **28**, 390 (2007) [arXiv:astro-ph/0702464].

[65] G. Gelmini, O. E. Kalashev and D. V. Semikoz, JCAP **0711**, 002 (2007) [arXiv:0706.2181 [astro-ph]].

- [66] A. M. Taylor and F. A. Aharonian, Phys. Rev. D **79**, 083010 (2009) [arXiv:0811.0396 [astro-ph]].
- [67] L. A. Anchordoqui, J. F. Beacom, H. Goldberg, S. Palomares-Ruiz and T. J. Weiler, Phys. Rev. Lett. **98**, 121101 (2007) [arXiv:astro-ph/0611580].
- [68] D. Hooper, A. Taylor and S. Sarkar, Astropart. Phys. **23**, 11 (2005) [arXiv:astro-ph/0407618].
- [69] M. Ave, N. Busca, A. V. Olinto, A. A. Watson and T. Yamamoto, Astropart. Phys. **23**, 19 (2005) [arXiv:astro-ph/0409316].
- [70] A. A. Abdo *et al.* [Fermi-LAT Collaboration], Phys. Rev. Lett. **104**, 101101 (2010) [arXiv:1002.3603 [astro-ph.HE]].
- [71] V. Berezinsky, A. Gazizov, M. Kachelriess and S. Ostapchenko, Phys. Lett. B **695**, 13 (2011) [arXiv:1003.1496 [astro-ph.HE]].
- [72] V. S. Berezinsky and A. Y. Smirnov, Astrophys. Space Sci. **32**, 461 (1975).
- [73] M. Ahlers, L. A. Anchordoqui, M. C. Gonzalez-Garcia, F. Halzen and S. Sarkar, Astropart. Phys. **34**, 106 (2010) [arXiv:1005.2620 [astro-ph.HE]].
- [74] M. Ahlers, L. A. Anchordoqui and A. M. Taylor, in preparation